Robust perpendicular exchange coupling in an ultrathin CoO/PtFe double layer: Strain and spin orientation

Anne D. Lamirand,[1] Márcio M. Soares,[1] Aline Y. Ramos,[1] Hélio C. N. Tolentino,[1,*] Maurizio De Santis,[1] Julio C. Cezar,[2] Abner de Siervo,[3] and Matthieu Jamet[4]

[1]*Institut Néel, CNRS and UJF, BP166, 38042 Grenoble, France*
[2]*Laboratório Nacional de Luz Síncrotron-LNLS, CP 6192, 13083-970 Campinas, Brazil*
[3]*Instituto de Física Gleb Wataghin, Universidade Estadual de Campinas-UNICAMP, 13083-970 Campinas, Brazil*
[4]*Institut Nanosciences et Cryogénie-INAC, CEA, 38042 Grenoble, France*

We report on the exchange coupling and magnetic properties of a strained ultrathin CoO/PtFe double layer with perpendicular magnetic anisotropy. The cobalt oxide growth by reactive molecular beam epitaxy on a Pt-terminated PtFe/Pt(001) surface gives rise to a hexagonal surface and a monoclinic distorted CoO 3 nm film at room temperature. This distorted ultrathin CoO layer couples with the PtFe(001) layer establishing a robust perpendicular exchange bias shift. Soft x-ray absorption spectroscopy provides a full description of the spin orientations in the CoO/PtFe double layer. The exchange bias shift is preserved up to the Néel antiferromagnetic ordering temperature of $T_N = 293$ K. This unique example of selfsame value for blocking and ordering temperatures, yet identical to the bulk ordering temperature, is likely related to the original strain-induced distortion and strengthened interaction between the two well-ordered spin layers.

The conception and optimization of tuned devices for spintronic applications[1] stir up a great interest in the exchange coupling between antiferromagnetic (AFM) and ferromagnetic (FM) layered materials[2–5] and, particularly, in the unidirectional anisotropy effect known as exchange bias (EB).[6] The AFM/FM exchange coupling relies on a variety of microscopic and atomic parameters, such as crystallographic order, surface morphology, strain effects, spin orientation, and competing anisotropies.[5] The EB effect is largely used to pin the FM magnetization along one orientation in a spin valve or magnetic tunnel junction.[1–5] It also provides the greatest opportunities to explore phenomena interlinking the spin and charge degrees of freedom[2] and, more recently, to control the electronic transport in a tunneling anisotropic magnetoresistance device.[3] In the latter the tunneling resistance is strongly affected by the orientation of the magnetic moments in the AFM layer, which can be partially rotated by the exchange coupling with the FM layer. Devices showing EB perpendicular to the layered surface are especially promising for low power consumption and ultrafast circuits, as well as for high-performance memories.[4,7]

Ultrathin CoO films number among the most interesting AFM layers for spintronic devices. At room temperature (RT), bulk CoO paramagnetic phase crystallizes in the rocksalt structure where pure Co and O planes alternate along the [111] axis (Fig. 1). It has a Néel temperature (T_N) of 293 K and a magnetic moment of 3.98 μ_B.[8,9] The magnetic moment lies far above the 3 μ_B value, revealing a large orbital contribution. The strong interaction between spin and orbital magnetic moments through the spin-orbit coupling drives the magnetic anisotropy energy.[10] Below T_N, the AFM ordering develops concomitantly with a monoclinic distorted phase.[9] The AFM structure is described as a stacking of FM hexagonal sheets of high-spin Co^{2+} ions coupled antiferromagnetically along the [111] direction. The spin structure is found collinear, with the moments close to the [001] axis of the rocksalt lattice (Fig. 1). The concomitant changes in the structure and magnetic

properties suggest that distortion and antiferromagnetism are linked by magnetostriction.[8–10] This view is supported by soft x-ray absorption spectroscopy (XAS) experiments in thin CoO layers grown on different substrates, which revealed significant modifications in the magnitude and orientation of the magnetic moments induced by epitaxial strain.[11] A critical issue for competitive CoO-based devices is, however, the preservation of a significant EB effect up to temperatures as close as possible to RT. Nevertheless, so far, all experimental studies in ultrathin (<10 nm) CoO/FM double-layer systems report EB blocking temperatures (T_B) smaller than T_N.[12–14] The situation seems to be identical for FM layers with planar or with perpendicular magnetic anisotropy (PMA).

We report here on the exchange coupling and magnetic properties of an ultrathin CoO/PtFe double layer. The growth by reactive molecular beam epitaxy of an ultrathin CoO on a Pt-terminated PtFe/Pt(001) surface leads to a hexagonal surface and monoclinic distorted CoO film at RT. The strain-induced monoclinic distortion in the CoO film accounts for its in-plane spin orientation. The exchange coupling of the distorted CoO layer with the PtFe(001) layer brings forth a robust perpendicular EB shift, which is preserved up to the AFM ordering temperature. This finding provides a unique example where the blocking (T_B) and ordering (T_N) temperatures are identical and match the bulk Néel temperature.

We have used *in situ* grazing incidence x-ray diffraction (GI-XRD) at the French CRG BM32 beamline at the European Synchrotron Radiation Facility (ESRF, France) to study and optimize the growth of ultrathin films on ultrahigh vacuum cleaned Pt(001) substrates.[15] Our Pt-terminated PtFe layer was grown by thermal deposition of three monolayers (ML) of Fe on a clean Pt(001) substrate hold at 600 K, followed by 1 ML Pt deposition. This procedure gives rise to a 1.2-nm-thick $L1_0$ PtFe(001) layer in coherent epitaxy on Pt(001). The $L1_0$ phase, formed by alternate Fe and Pt atomic planes along the c axis of the tetragonal structure, provides an out-of-plane spin
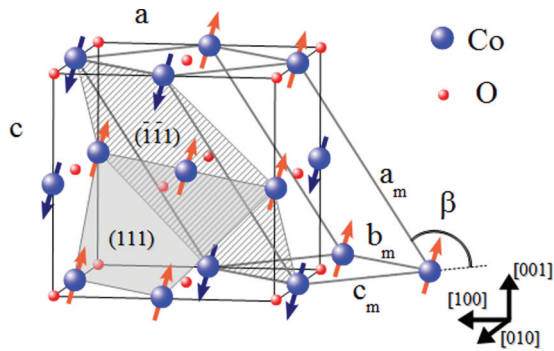
FIG. 1. (Color online) CoO rocksalt (a, c) and monoclinic (a_m, b_m, c_m, β) unit cell parameters and low-temperature AFM spin structure (Ref. 9). The gray half-hexagon indicates Co FM sheets on (111) planes, antiparallel along the [111] direction. The hatched hexagon indicates Co AFM sheets on ($\bar{1}\bar{1}1$) planes.

network with strong perpendicular magnetic anisotropy.[16,17] The CoO layer was grown by reactive molecular beam epitaxy on the ultrathin PtFe(001) layer hold at 523 K. Owing to the high oxidation potential of Fe,[18] reactive CoO deposition on pure Fe oxidizes about 1–2 ML of Fe.[18–20] Our Pt-terminated high-quality PtFe(001) layer shows a small oxide contribution, likely related to Fe atoms dispersed within the CoO layer or from Fe-O bounds at the interface. We show here below that the magnetic properties are characteristic of metallic $L1_0$ PtFe and are not affected by the small oxide contribution. CoO thickness was chosen around 3 nm, close to the onset thickness for frozen AFM spins.[19] The detailed growth procedure and x-ray diffraction study of CoO on both PtFe(001) and Pt(001) will be presented elsewhere.[21]

The GI-XRD analysis at RT shows that hexagonal Co atomic planes sit on the underlying Pt-terminated square network [Fig. 2(a)]. Such a hexagonal (111)-like CoO surface is not uncommon on substrates with similar lattice misfit between the oxide and substrate.[22] The 2D-rectangle network (a_m, b_m) corresponding to CoO(111) hexagonal planes does not exactly match the 2D-rectangle network ($2a_{Pt}/\sqrt{2}$, $a_{Pt}/\sqrt{2}$) defined by the Pt underlayer. The misfits along a_m and b_m axis ([112] and [1$\bar{1}$0] rocksalt directions) are
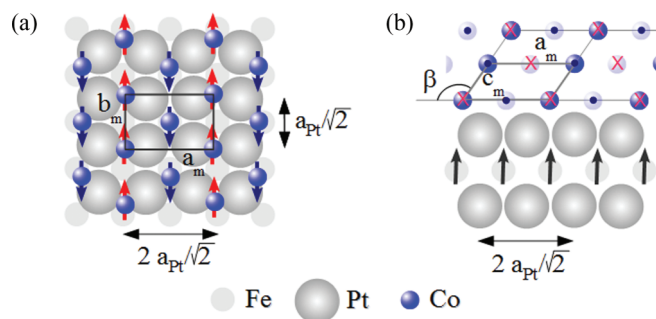

FIG. 2. (Color online) Illustration of the hexagonal (111)-like CoO layer on PtFe/Pt(001). Spin orientation and relation between the CoO monoclinic (a_m, b_m, c_m, β) and Pt (a_{Pt}) parameters. (a) Top view: Co AFM spin structure (Fig. 1) projected onto the surface, with spin axis along the [1$\bar{1}$0] direction. (b) Side view: Fe spins are perpendicular to the surface and the projected Co AFM spins point forward ($\bullet$) or backward ($\times$).

$\epsilon_a = -6.1\%$ and $\epsilon_b = +8.6\%$, respectively, bringing about a slightly anisotropic stress. Consequently, the 3-nm-thick CoO layer is slightly compressed and develops a small monoclinic distortion ($\beta \neq \beta_o = 125.264°$). About 8-nm-large well-crystallized domains are observed for the four orientations allowed by symmetry.[21] The RT monoclinic cell parameters obtained from GI-XRD analysis averaged over all domains are $a_m = 5.220(2)$ Å, $b_m = 3.005(1)$ Å, $c_m = 2.995(3)$ Å, and $\beta = 124.995(5)°$. In the slightly deformed tetragonal lattice, the parameters are $a = 4.243(3)$ Å and $c = 4.272(3)$ Å.

Element-resolved spin orientation of the CoO/PtFe/Pt(001) system was *ex situ* investigated by XAS, using linear and circular magnetic dichroism at Fe and Co $L_{2,3}$ edges. XAS measurements under applied magnetic field were performed at the PGM beamline of the Laboratório Nacional de Luz Síncrotron (LNLS, Brazil), with a spectral resolution of $E/\Delta E = 6000$ and degrees of linear and circular polarizations close to 100% and 80%, respectively. The sample was allowed to rotate about a vertical axis, with the polar angle θ defined as the angle between the surface normal and the x-ray propagation. X-ray linear dichroism (XLD) was taken with linear horizontal polarization, as the difference between XAS recorded at θ and $\theta = 0°$. X-ray magnetic circular dichroism (XMCD) was taken as difference between right and left circular polarizations at $\theta = 0°$. All spectra were collected using total electron yield, corrected for electron yield saturation effects[18] and normalized far from $L_{2,3}$ edges. The XAS study has been complemented by polar magneto-optic Kerr effect (MOKE) measurements. All magnetic measurements were performed after a field cooling from 350 K down to 5 K under an applied magnetic field of +5 kOe along the normal to the sample surface.

Figure 3(a) shows the Co $L_{2,3}$ XAS spectra at 5 K for $\theta = 0°$ and $\theta = 70°$. The difference between them gives a clear XLD signal, which essentially measures the charge anisotropy associated with both the local crystal field and the local exchange field through the spin-orbit coupling.[11,19,23] The latter contribution is known as x-ray magnetic linear dichroism (XMLD). Following Wu and coworkers[19] we used the intensity ratio RL_3 between the peaks at 778.74 eV (C) and 778.26 eV (B) as a measure of the overall anisotropy. The XMLD contribution to RL_3 is maximum at the angle where the polarization vector is perpendicular to the Co magnetic moments.[19,23] A $\cos^2 \theta$ fit of RL_3 for the low-temperature measurements [inset Fig. 3(a)] has its minimum when the polarization is parallel to the surface ($\theta = 0°$) and its maximum at about $\theta = 90°$, within an accuracy of a few degrees. We can then conclude that the Co spin axis is essentially parallel to the surface. As the Fe spin axis is perpendicular to the surface, the coupling between Co and Fe spins through the Pt interface layer is at 90° (Fig. 2). Further information on the spin orientation within the film plane can be sought from the rich manifold peak structure, including the L_3 and L_2 Co edges. Atomic multiplet calculations performed by van der Laan and coworkers[23] show that Co magnetization axis with respect to the crystalline axis can be differentiated from the relative variations of L_3 and L_2 features and from those of L_3 A (at 777.0 eV) and C peaks (Fig. 5 in Ref. 23). The XLD signal in Fig. 3(a) matches the situation where Co spins are along the b_m axis ([1$\bar{1}$0] direction) (Fig. 2).
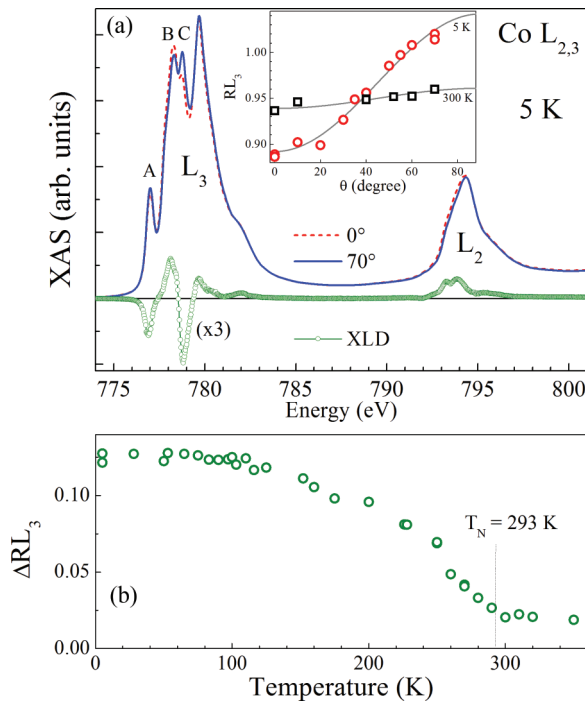
FIG. 3. (Color online) (a) Co $L_{2,3}$ XAS spectra of a 3-nm-thick CoO layer on PtFe/Pt(001) at 5 K after cooling in a +5 kOe magnetic field. Linear polarization parallel to the surface [$\theta = 0°$, dashed (red) line] and towards the surface normal [$\theta = 70°$, solid (blue) line]. The XLD [dot (green) line] is the difference between them. The angle-dependent anisotropy, defined by the C over B peak contrast, is shown in the inset. (b) Temperature dependence of the anisotropy.
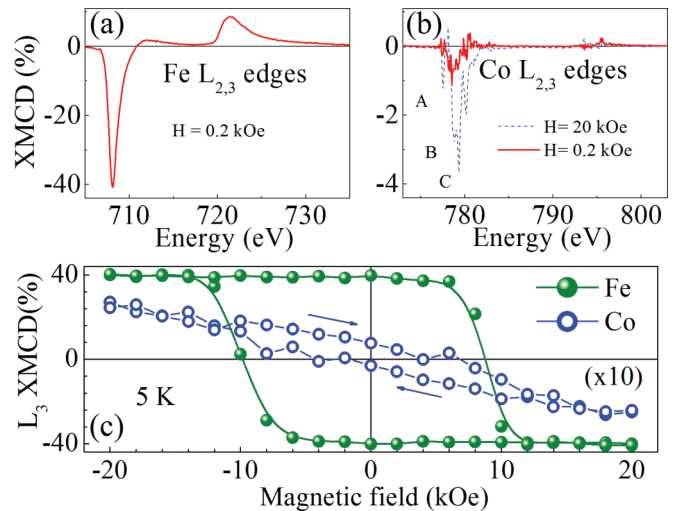

FIG. 4. (Color online) (a) Fe $L_{2,3}$ and (b) Co $L_{2,3}$ XMCD: Solid (red) lines are close to remanence; dashed (blue) line is at 20 kOe. Note the factor of ten between scales. (c) Element-selective hysteresis loops at Fe and Co L_3 edges.

As a small out-of-plane contribution of interface Co spin cannot be ruled out from the only XMLD, we went on performing XMCD measurements at Fe and Co $L_{2,3}$ edges (Fig. 4). Element-selective hysteresis loops were drawn by reporting for each value of the applied perpendicular magnetic field the maximum amplitude of the XMCD at the Fe and Co L_3 edges. Fe $L_{2,3}$ XMCD at 5 K [Fig. 4(a)] has a metallic signature and a maximum amplitude of about 40% at the L_3 edge. The Fe hysteresis loop is shifted towards negative values and yields a magnetization at zero field (remanence) close to the saturation magnetization [Fig. 4(c)]. Such almost 100% remanence indicates the PMA character of the PtFe layer, which has been confirmed by a hysteresis loop measured at $\theta = 70°$ (not shown). At the Co L_3 edge, we observe a weak XMCD signal due to the Co spin component not compensated by AFM interactions [Fig. 4(b)]. It shows the CoO characteristic multiplet features.[20,23] The maximum amplitude of this XMCD signal is roughly proportional to the applied magnetic field but shows a weak hysteresis opening with a remaining contribution of about 0.5(3)% close to remanence and coinciding with the Fe hysteresis loop [Fig. 4(c)]. Two contributions to the field-dependent Co XMCD should then be considered. The linear contribution is a bulk-like effect, arising from the coupling of the whole set of Co spins in the CoO layer to the external magnetic field. On the other hand, the weak hysteresis, following the Fe hysteresis loop, results from an interface exchange coupling with Fe. This small contribution originates

from an uncompensated Co spin component perpendicular to the surface. It is worth noting that the Co hysteresis loop shows an upward shift of about 0.3% that could be related to exchange bias. However, this shift is close to the experimental accuracy and further measurements would be necessary to properly address this point.

We turn now to the temperature-dependent magnetic properties. In the RL_3 ratio [Fig. 3(a)], the magnetic and structural contributions to the XLD signal are mixed up by the local tetragonal crystal field. This explains the small residual anisotropy observed at 300 K [Fig. 3(a), inset], where no magnetic contribution is expected. Magnetic and nonmagnetic contributions can be disentangled by a full temperature dependence study of the anisotropy amplitude, experimentally defined as $\Delta RL_3 = RL_3(70°) - RL_3(0°)$. ΔRL_3 decreases following a Brillouin-like function up to $T_N \approx 293$ K and then stabilizes [Fig. 3(b)]. This unambiguously confirms that the AFM order is preserved up to about 293 K. It also proves that the Néel temperature of the CoO film is very close to that of the bulk CoO crystal.[9] Above T_N only the nonmagnetic crystal field contribution to the anisotropy still remains.

We will now focus on the temperature dependence of the coercive field (H_C) and exchange bias shift (H_{EB}) measured by polar MOKE (Fig. 5). The hysteresis loop shows 100% remanence from the lowest to the highest temperature (Fig. 5, inset), confirming that the PMA of the ultrathin PtFe layer is preserved. The loops also show a perpendicular exchange bias shift up to the nominal bulk Néel temperature [Fig. 5(b)], asserting the steadfastness of the CoO/PtFe exchange interfacial coupling and also of the AFM order of the CoO layer. The exchange bias shift is about $H_{EB} = -0.75$ kOe at 5 K.

In low-temperature bulk CoO, the monoclinic distortion is essentially driven by the Jahn-Teller effect due to the partial filling of the Co^{2+} t_{2g} orbitals.[10] It can be seen as the result of a main tetragonal plus a small trigonal distortion.
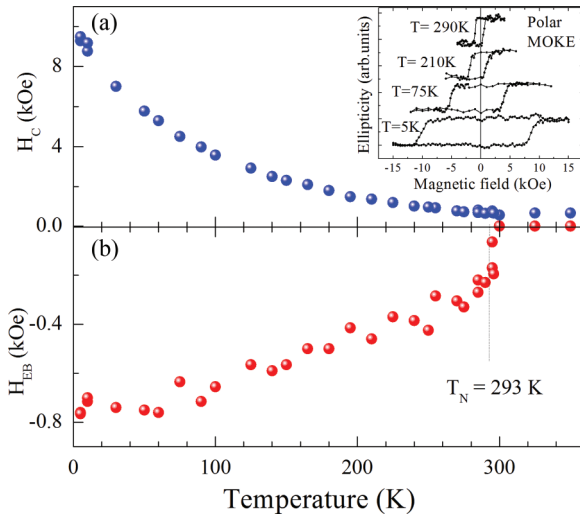
FIG. 5. (Color online) Temperature dependence of the (a) coercive field and (b) exchange bias after cooling the sample in a +5 kOe perpendicular magnetic field. Polar MOKE hysteresis loops at a few selected temperatures are shown in the inset.

The magnetic dipole-dipole interaction tends to align spins in the (111) plane, while crystal field energy, arising from the compressive ($c/a < 1$) tetragonal deformation, favors the [001] direction.[8] As a consequence, the CoO spin structure is collinear with the spin axis making a small angle with the [001] direction of the rocksalt lattice[8,9] (Fig. 1). In epitaxial thin films the strain drives the anisotropy. Csiszar and coworkers[11] have shown that an ultrathin CoO layer sandwiched by MnO layers on Ag(001) shows an out-of-plane magnetization axis along [001], while in direct epitaxy the Ag(001) substrate shows an in-plane magnetization axis orthogonal to the [001] direction. The main structural difference between the two cases lies in the CoO(001) epitaxial strain, which is tensile on MnO(001) and slightly compressive on Ag(001), generating respectively a compressive ($c/a < 1$) and a slightly extensive ($c/a > 1$) tetragonal deformation. The slightly anisotropic strain imposed by the PtFe/Pt(001) surface on the CoO layer leads to a monoclinic distorted lattice that resembles that of bulk CoO at low temperatures. However, while the tetragonal deformation is compressive in the bulk ($c/a = 0.988$), it is extensive in the film ($c/a = 1.008$). In this particular situation, the dipole-dipole magnetic energy is minimized when the FM Co spins are within the (111) plane and parallel to the [1$\bar{1}$0] direction.[24]

It is noteworthy that, owing to the monoclinic distortion, the hexagonal (111) plane perpendicular to the trigonal distortion is no longer equivalent to the other hexagonal planes. From strict structural considerations, we can identify the hexagonal plane sitting on the PtFe(001) surface as the one parallel to the (a_m, b_m) plane and not the one perpendicular to the trigonal elongation [Fig. 1, hatched ($\bar{1}\bar{1}1$) and gray (111) hexagons, respectively]. It is then expected that the Co sheets parallel to the surface will be those containing fully compensated spins (Fig. 2). In this plane rows of Co spins are coupled ferromagnetically along b_m ([1$\bar{1}$0] direction) and antiferromagnetically along a_m ([112] direction). Such AFM configuration resembles the model predicted by DFT

calculations for a single CoO overlayer on Ir(001).[22] The Co spin orientation (Fig. 2) deduced from our XLD analysis is fully consistent with the sequence of alternate FM Co(111) planes, but the spin axis here is along the [1$\bar{1}$0] direction and does not contain any component out of the hexagonal surface.

Many experimental studies report that to reach blocking (T_B) temperatures close to T_N, CoO thickness should be at least about 10 nm.[5,12,25,26] In most cases, the blocking temperature measured from the onset of the exchange bias shift is smaller than the expected T_N. Films with thickness around 3–5 nm display T_B typically around 200–240 K. In contrast, our CoO layer sustains an EB shift up to $T_N \approx 293$ K. This exceptional behavior must be related to the good crystalline quality and to the stable spin configuration at the interface. It demonstrates that AFM order as in the bulk may be established in CoO films as thin as 3 nm and that the thickness effect, which reduces the ordering temperature, is not an intrinsic property.

CoO layers may couple with FM layers showing in-plane[12,19,20] or out-of-plane[13,14] anisotropy. Exchange coupling properties are largely determined by the direction and strength of the anisotropy in the FM and in the AFM layers. The XMCD study reveals that there is at the interface a weak uncompensated Co spin component perpendicular to the surface. However, Co spins are essentially aligned in-plane. The coupling between interfacial Co and Fe spins is then at 90° [Fig. 2(b)]. A similar 90° coupling is not unusual and has been reported for in-plane anisotropy systems as CoO/Fe on Ag(001).[19] Such an orthogonal coupling minimizes the energy for a fully compensated AFM interfacial spin configuration interacting with the exchange field of the FM layer. In addition, we should recall that in the PtFe layer the high magnetic anisotropy relies on the strong spin-orbit coupling of the Pt site and hybridization between Fe $3d$ and Pt $5d$ states.[27] Exchange coupling of Co and Fe moments through Pt $5d$ states at the interface likely contributes to the preservation of the EB shift up to the AFM phase transition.

To summarize, the growth by reactive molecular beam epitaxy of a 3-nm-thick CoO layer on a Pt(001)-terminated PtFe(001) surface gives rise to a hexagonal CoO(111)-like surface, which develops into a monoclinic distorted film at RT. Using polarization-dependent XAS at Co and Fe $L_{2,3}$ edges, we have given a complete description of the orientation of the Co and Fe magnetic moments. We have shown that the coupling of such a distorted CoO hexagonal layer with PMA PtFe(001) brings forth a very robust perpendicular exchange bias shift preserved up to the antiferromagnetic ordering temperature of 293 K. This is a unique example where the blocking and Néel temperatures for an ultrathin CoO layer are identical and match the bulk Néel temperature. Such exceptional behavior shares a close relationship with the strain-induced distortion of the oxide layer. Our outcome demonstrates that the thickness effect on T_N, which reduces the ordering temperature, and reduction of blocking temperature (T_B) are not intrinsic properties of these double layers.

*helio.tolentino@grenoble.cnrs.fr

[1] C. Chappert, A. Fert, and F. Nguyen van Dau, Nat. Mater. **6**, 813 (2007).

[2] X. He, Y. Wang, N. Wu, A. Caruso, E. Vescovo, K. Belashchenko, P. Dowben, and C. Binek, Nat. Mater. **9**, 579 (2010).

[3] B. Park, J. Wunderlich, X. Marti, V. Holy, Y. Kurosaki, M. Yamada, H. Yamamoto, A. Nishide, J. Hayakawa, H. Takahashi, A. Shick, and T. Jungwirth, Nat. Mater. **10**, 347 (2011).

[4] Y. Shiratsuchi, H. Noutomi, H. Oikawa, T. Nakamura, M. Suzuki, T. Fujita, K. Arakawa, Y. Takechi, H. Mori, T. Kinoshita, M. Yamamoto, and R. Nakatani, Phys. Rev. Lett. **109**, 077202 (2012).

[5] A. E. Berkowitz and K. Takano, J. Magn. Magn. Mater. **200**, 552 (1999).

[6] W. H. Meiklejohn and C. P. Bean, Phys. Rev. **102**, 1413 (1956).

[7] S. Mangin, D. Ravelosona, J. Katine, M. Carey, B. Terris, and E. Fullerton, Nat. Mater. **5**, 210 (2006).

[8] W. L. Roth, Phys. Rev. **110**, 1333 (1958).

[9] W. Jauch, M. Reehuis, H. J. Bleif, F. Kubanek, and P. Pattison, Phys. Rev. B **64**, 052102 (2001).

[10] A. Schrön, C. Rödl, and F. Bechstedt, Phys. Rev. B **86**, 115134 (2012).

[11] S. I. Csiszar, M. W. Haverkort, Z. Hu, A. Tanaka, H. H. Hsieh, H.-J. Lin, C. T. Chen, T. Hibma, and L. H. Tjeng, Phys. Rev. Lett. **95**, 187205 (2005).

[12] P. J. van der Zaag, Y. Ijiri, J. A. Borchers, L. F. Feiner, R. M. Wolf, J. M. Gaines, R. W. Erwin, and M. A. Verheijen, Phys. Rev. Lett. **84**, 6102 (2000).

[13] S. Maat, K. Takano, S. S. P. Parkin, and E. E. Fullerton, Phys. Rev. Lett. **87**, 087202 (2001).

[14] J. M. Tonnerre, M. De Santis, S. Grenier, H. C. N. Tolentino, V. Langlais, E. Bontempi, M. García-Fernández, and U. Staub, Phys. Rev. Lett. **100**, 157202 (2008).

[15] M. M. Soares, M. De Santis, H. C. N. Tolentino, A. Y. Ramos, M. El Jawad, Y. Gauthier, F. Yildiz, and M. Przybylski, Phys. Rev. B **85**, 205417 (2012).

[16] S. Okamoto, N. Kikuchi, O. Kitakami, T. Miyazaki, Y. Shimada, and K. Fukamichi, Phys. Rev. B **66**, 024413 (2002).

[17] M. M. Soares, H. C. N. Tolentino, M. D. Santis, A. Y. Ramos, and J. C. Cezar, J. Appl. Phys. **109**, 07D725 (2011).

[18] T. J. Regan, H. Ohldag, C. Stamm, F. Nolting, J. Lüning, J. Stöhr, and R. L. White, Phys. Rev. B **64**, 214422 (2001).

[19] J. Wu, J. S. Park, W. Kim, E. Arenholz, M. Liberati, A. Scholl, Y. Z. Wu, C. Hwang, and Z. Q. Qiu, Phys. Rev. Lett. **104**, 217204 (2010).

[20] R. Abrudan, J. Miguel, M. Bernien, C. Tieg, M. Piantek, J. Kirschner, and W. Kuch, Phys. Rev. B **77**, 014411 (2008).

[21] A. D. Lamirand, M. M. Soares, M. D. Santis, A. Y. Ramos, and H. C. N. Tolentino (unpublished).

[22] F. Mittendorfer, M. Weinert, R. Podloucky, and J. Redinger, Phys. Rev. Lett. **109**, 015501 (2012).

[23] G. van der Laan, E. Arenholz, R. V. Chopdekar, and Y. Suzuki, Phys. Rev. B **77**, 064407 (2008).

[24] M. Finazzi and S. Altieri, Phys. Rev. B **68**, 054420 (2003).

[25] T. Ambrose and C. L. Chien, Phys. Rev. Lett. **76**, 1743 (1996).

[26] M. Molina-Ruiz, A. F. Lopeandía, F. Pi, D. Givord, O. Bourgeois, and J. Rodríguez-Viejo, Phys. Rev. B **83**, 140407 (2011).

[27] N. Nakajima, T. Koide, T. Shidara, H. Miyauchi, H. Fukutani, A. Fujimori, K. Iio, T. Katayama, M. Nývlt, and Y. Suzuki, Phys. Rev. Lett. **81**, 5229 (1998).